Nuclear magnetic resonance study of anion and cation dynamics in CsSiH$_3$

R.V. Skoryunov [a], O.A. Babanova [a], A.V. Soloninin [a], A.V. Skripov [a, *], J.-N. Chotard [b], R. Janot [b], W.S. Tang [c, d, e], M. Dimitrievska [c, f], T.J. Udovic [c]

[a] Institute of Metal Physics, Ural Branch of the Russian Academy of Sciences, Ekaterinburg 620108, Russia
[b] Laboratoire de Réactivité et Chimie des Solides (LRCS), UMR 7314 CNRS, Université de Picardie Jules Verne, 80039 Amiens Cedex, France
[c] NIST Center for Neutron Research, National Institute of Standards and Technology, Gaithersburg, MD 20899-6102, USA
[d] Department of Materials Science and Engineering, University of Maryland, College Park, MD 20742-2115, USA
[e] Geophysical Laboratory, Carnegie Institution of Washington, Washington, DC 20015, USA
[f] National Renewable Energy Laboratory, Golden, CO 80401, USA

ABSTRACT

In order to study the dynamical properties of cesium silanide CsSiH$_3$, we have measured the ^{1}H and ^{133}Cs nuclear magnetic resonance (NMR) spectra and spin-lattice relaxation rates in this compound over the temperature range of 5–354 K. The results of the ^{1}H NMR measurements indicate that [SiH$_3$]$^-$ anions in CsSiH$_3$ retain unusually high reorientational mobility down to low temperatures. In particular, a significant narrowing of the proton NMR spectrum due to [SiH$_3$]$^-$ reorientations is observed in the range ~ 10–14 K. The order-disorder ($\beta \rightarrow \alpha$) phase transition accompanied by the strong acceleration of [SiH$_3$]$^-$ reorientations and by the change in the reorientational mechanism is observed above 200 K; according to the ^{1}H spin-lattice relaxation data, this transition appears to be gradual. For the high-temperature disordered α-phase, the activation energy for [SiH$_3$]$^-$ reorientations is found to be 41(4) meV. The ^{133}Cs NMR results are consistent with the onset of diffusive motion of Cs$^+$ cations at the frequency scale of ~10^4 s^{-1} above 300 K.

© 2018 Elsevier B.V. All rights reserved.

1. Introduction

Alkali-metal silanides MSiH$_3$ (M = K, Rb, Cs) consisting of M^+ cations and pyramidal [SiH$_3$]$^-$ anions have received significant recent attention as potential hydrogen-storage materials [1–5]. These compounds can be prepared by reversible hydrogenation of Zintl phases MSi with the equilibrium hydrogen gas pressure of 0.1 MPa near 410 K [3]. Above 300 K, the crystal structure of all three MSiH$_3$ compounds is cubic (α-phase, space group $Fm\bar{3}m$) with NaCl-type arrangement of M^+ cations and orientationally disordered [SiH$_3$]$^-$ anions. At lower temperatures, these disordered α-phases are transformed into the ordered β-phases with orthorhombic (β-KSiH$_3$, space group $Pnma$) or monoclinic (β-RbSiH$_3$ and β-CsSiH$_3$, space group $P2_1/m$) structures [3,6,7]. The corresponding entropy-driven $\alpha \leftrightarrow \beta$ phase transitions are found to be reversible, but hysteretic [7,8].

It is known that in many complex hydrides, the reorientational motion of complex anions (such as [BH$_4$]$^-$, [AlH$_4$]$^-$, [NH$_2$]$^-$, [B$_{12}$H$_{12}$]$^{2-}$) [9–13] strongly contributes to the balance of energies determining the thermodynamic stability of these compounds; therefore, information on the anion reorientational dynamics is important for understanding the fundamental properties of complex hydrides. The first evidence of the reorientational motion of [SiH$_3$]$^-$ anions in alkali-metal silanides was obtained in the wide-line nuclear magnetic resonance (NMR) study [14] that revealed the narrowing of the ^{1}H NMR spectrum of KSiH$_3$ above 170 K. The motional narrowing of the ^{2}D NMR spectrum was also observed for deuterium-substituted KSiD$_3$ and RbSiD$_3$ above 200 K [8]. Recent quasielastic neutron scattering (QENS) measurements [7,8,15,16] have shown that phase transitions from the ordered β-phases of MSiH$_3$ to the disordered α-phases are accompanied by the strong acceleration of anion reorientations. Typical reorientational jump rates for α-phases of all MSiH$_3$ compounds just above room temperature are of the order of 10^{12} s^{-1}. It is interesting to note that similar order-disorder phase transitions accompanied by an acceleration of anion reorientations have been found to occur in a

number of complex hydrides, including the family of alkali-metal *closo*-hydroborates with $[B_{12}H_{12}]^{2-}$ and $[B_{10}H_{10}]^{2-}$ anions [13,17–19]. The high-temperature disordered phases of lithium and sodium *closo*-hydroborates and their derivatives exhibit extremely high Li^+ and Na^+ ionic conductivities [19–21], which are believed to be related [22–24] to fast anion reorientations. For alkali-metal silanides, a possible relation between anion reorientations and cation diffusion has not been studied so far.

In the present work, we use nuclear magnetic resonance measurements of ^1H and ^{133}Cs spectra and spin-lattice relaxation rates to investigate both the reorientational motion of $[SiH_3]^-$ anions and the diffusive motion of Cs^+ cations in $CsSiH_3$ over wide temperature ranges. The results of this first NMR study of $CsSiH_3$ indicate that $[SiH_3]^-$ reorientations in β-$CsSiH_3$ are unusually fast, and on the frequency scale of 10^5 s^{-1} they are not "frozen out" down to very low temperatures. The diffusive motion of Cs^+ cations becomes observable at the NMR frequency scale in α-$CsSiH_3$ above 300 K.

2. Experimental details

$CsSiH_3$ sample was prepared by the direct solid − gas reaction between CsSi and H_2, as described in Ref. [3]. The Zintl phase CsSi was synthesized by high-temperature annealing of a 1:1.03 mixture of cesium (99.8%, Alfa Aesar [25]) and silicon (powder, −325 mesh, Sigma Aldrich). All materials were handled in an argon-filled glovebox. The mixture was arc-weld-sealed within a stainless-steel ampule inside the glovebox. The ampule was heated to 873 K and kept at this temperature for 48 h. Then it was cooled with the rate of 0.2 K/min down to room temperature. A slight excess of silicon was added to ensure a complete reaction of the starting cesium. The resulting CsSi compound was first activated via evacuation at 473 K for 12 h and then hydrogenated at 373 K with ~5 MPa of hydrogen for 24 h. For NMR experiments, the powdered $CsSiH_3$ sample was flame-sealed in a glass tube under ~0.5 bar of nitrogen gas.

Low-field ^1H NMR measurements were performed on a pulse spectrometer with quadrature phase detection at the frequencies $\omega/2\pi = 28$ and 90 MHz. The magnetic field was provided by a 2.1 T iron-core Bruker magnet. A home-built multinuclear continuous-wave NMR magnetometer working in the range 0.32–2.15 T was used for field stabilization. For rf pulse generation, we used a home-built computer-controlled pulse programmer, a PTS frequency synthesizer (Programmed Test Sources, Inc.) and a 1 kW Kalmus wideband pulse amplifier. A probehead with the sample was placed into an Oxford Instruments CF1200 continuous-flow cryostat using nitrogen or helium as a cooling agent. The sample temperature monitored by a chromel − (Au-Fe) thermocouple was stable to ±0.1 K. High-field ^{133}Cs NMR measurements were performed on a Bruker AVANCE III 500 spectrometer at the frequency $\omega/2\pi = 65.62$ MHz. Typical values of the $\pi/2$ pulse length were 3–4 μs for both ^1H and ^{133}Cs. All the NMR measurements were performed with increasing temperature and with 15 min stabilization time at each temperature prior to a measurement. Nuclear spin-lattice relaxation rates were measured using the saturation − recovery method. NMR spectra were recorded by Fourier transforming the solid echo signals (pulse sequence $\pi/2_x − t − \pi/2_y$ with $t = 20–22$ μs).

3. Results and discussion

3.1. ^1H NMR spectra and spin-lattice relaxation rates

The evolution of the proton NMR spectra for $CsSiH_3$ with temperature is shown in Fig. 1. As can be seen from this figure, the spectra exhibit a considerable narrowing with increasing temperature. Fig. 2 shows the temperature dependence of the line width
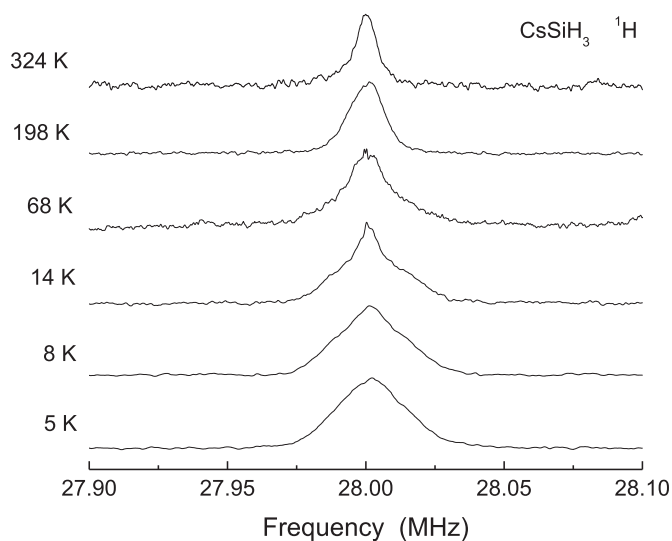

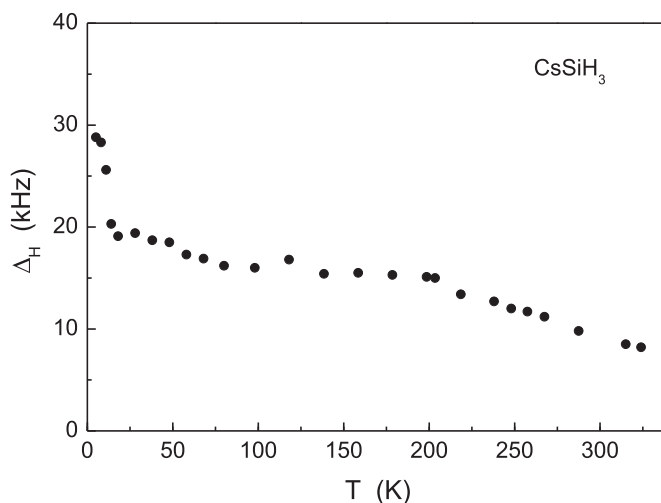Fig. 1. Evolution of the proton NMR spectrum for $CsSiH_3$ with temperature.

Fig. 2. Temperature dependence of the width (full width at half-maximum) of the ^1H NMR spectrum measured for $CsSiH_3$ at 28 MHz.

Δ_H (full width at half-maximum). At low temperatures, the width of the ^1H NMR spectrum is determined by dipole-dipole interactions between static nuclear spins; this is the 'rigid-lattice' line width Δ_{HR}. A rough theoretical estimate of Δ_{HR} can be obtained from the second moment calculations using the structural data for β-$CsSiH_3$ [3], see Fig. 3. The calculated 'rigid-lattice' second moment of the ^1H NMR line for β-$CsSiH_3$ is 5.2×10^9 s^{-2}. Assuming a Gaussian shape of the spectrum, this second moment should correspond to the Δ_{HR} value of 27.1 kHz. The experimental Δ_H value at $T = 5$ K (28.8 kHz) is close to this estimate.

With increasing temperature, the line width starts to decrease, since the onset of H jump motion leads to a partial averaging of dipole-dipole interactions. Such motional narrowing is expected to be substantial at the temperature at which the H jump rate τ^{-1} becomes nearly equal to $2\pi\Delta_{HR}$ [26]; for β-$CsSiH_3$, this characteristic frequency is about 1.7×10^5 s^{-1}. As can be seen from Fig. 2, a considerable line narrowing in β-$CsSiH_3$ is observed already at 14 K. This means that SiH_3 groups in the cesium silanide retain high reorientational mobility down to very low temperatures. For comparison, the onset of the proton NMR line narrowing in β-$KSiH_3$
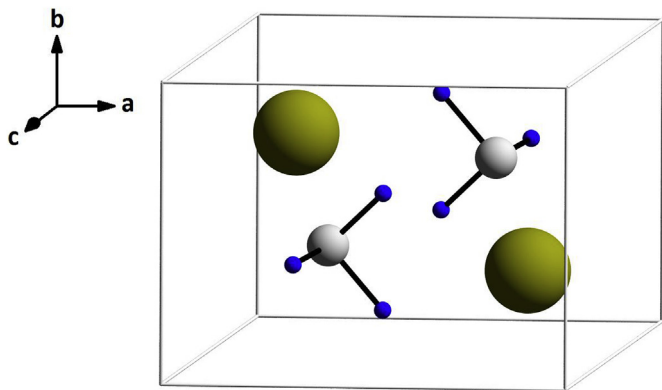
Fig. 3. Schematic view of the structure of β-CsSiH₃. Olive spheres: Cs atoms; gray spheres: Si atoms; blue spheres: H atoms. (For interpretation of the references to colour in this figure legend, the reader is referred to the Web version of this article.)

occurs near 170 K [14]. Recent QENS studies of MSiH₃ compounds [16] have shown that the reorientational SiH₃ motion in β-CsSiH₃ is much faster than in β-KSiH₃ and β-RbSiH₃. However, because of the limited energy resolution of QENS measurements, they can only probe the jump rates down to ~4 × 10⁸ s⁻¹ (for β-CsSiH₃, this low limit corresponds to the temperature of about 140 K [16]). Since NMR measurements are sensitive to much slower jump rates, they allow us to trace the reorientational motion down to lower temperatures. An Arrhenius extrapolation of the QENS results for β-CsSiH₃ [16] to the low-T region indicates that the H jump rate of 10⁵ s⁻¹ is expected to occur near 73 K. Thus, SiH₃ reorientations are not "frozen out" at the frequency scale of 10⁵ s⁻¹ down to much lower temperatures than those expected on the basis of extrapolation of the QENS data. It should be noted that, although the low-T reorientational SiH₃ motion in CsSiH₃ is unusually fast, it cannot be treated in terms of the rotational tunneling [27], since the value of Δ$_H$ at the lowest temperature corresponds to the calculated 'rigid-lattice' limit. In the known cases of the rotational tunneling [27], Δ$_H$ at the lowest temperatures is considerably smaller than this 'rigid-lattice' value.

As can be seen from Fig. 2, in the temperature range of 100–200 K, the value of Δ$_H$ remains nearly constant. This plateau regime is related to the fact that even when τ^{-1} is much higher than 2πΔ$_{HR}$, a localized H motion (such as reorientational motion) leads to only partial averaging of the dipole-dipole interactions. The plateau value of Δ$_H$ should depend on the mechanism of reorientations. For β-CsSiH₃, the second moment of the proton NMR line is dominated by ¹H − ¹H interactions within the same SiH₃ group (the 'intramolecular' contribution). A fast uniaxial rotation of SiH₃ group around the 3-fold symmetry axis is expected to result in a 75% drop of this contribution to the second moment with respect to its 'rigid-lattice' value [14,28]. Assuming that the line shape is Gaussian, this corresponds to a 50% drop of the line width. The experimental plateau value of Δ$_H$ for β-CsSiH₃ (~15 kHz) is indeed close to one-half of the low-temperature value; this is consistent with the model of uniaxial reorientations, in agreement with the QENS results for β-phases of MSiH₃ [16]. The additional decrease in the line width above 220 K (Fig. 2) can be attributed to the change in the reorientational mechanism related to the β → α phase transition [16]. QENS data for the orientationally-disordered α-phases of MSiH₃ [7,15,16] are consistent with the reorientational mechanism in which each H atom traverses many sites on the surface of a sphere roughly centered on the Si atom. The effects of such nearly isotropic reorientational motion on Δ$_H$ can be estimated in the following way. Since fast isotropic rotations should

average out the dipole-dipole interactions within SiH₃ groups, we have to calculate only the 'intermolecular' contribution to the second moment (between different SiH₃ groups and between SiH₃ groups and ¹³³Cs spins). This contribution can be roughly estimated by placing all protons in each SiH₃ group to its center (Si atom) and taking into account only the distances between centers of different groups [10]. The second moment for α-CsSiH₃ calculated using this approach is 4.1×10^8 s⁻²; for a Gaussian shape of the proton NMR line, this value corresponds to the line width of 7.6 kHz. The experimental value of Δ$_H$ at the high-temperature end of our measurements (8.2 kHz) is close to this estimated level.

The behavior of the proton spin-lattice relaxation rates R_1^H measured at two resonance frequencies ($\omega/2\pi = 28$ and 90 MHz) is shown in Fig. 4. We have not found any significant deviations from a single-exponential recovery of the nuclear magnetization over the entire temperature range studied. General features of the observed temperature dependence of R_1^H are typical of complex hydrides with reorienting anions [9], where the dominant relaxation mechanism is related to motional modulation of the dipole-dipole interaction between nuclear spins. For this mechanism, the proton spin-lattice relaxation rate exhibits a peak at the temperature at which the reorientational jump rate τ^{-1} becomes nearly equal to the nuclear magnetic resonance frequency ω. According to the standard theory [26], in the limit of slow motion ($\omega\tau \gg 1$), R_1^H is proportional to $\omega^{-2}\tau^{-1}$, and in the limit of fast motion ($\omega\tau \ll 1$), R_1^H is proportional to τ being frequency-independent. If the temperature dependence of the jump rate τ^{-1} follows the Arrhenius law with the activation energy E_a,

$$\tau^{-1} = \tau_0^{-1} \exp(-E_a/k_B T), \qquad (1)$$

a plot of ln R_1^H versus T^{-1} is expected to be linear in the limits of both slow and fast motion with the slopes of $-E_a/k_B$ and E_a/k_B, respectively. We have verified that there are no additional R_1^H peaks below 80 K; the relaxation rate continues to decrease with decreasing temperature. As can be seen from Fig. 4, the observed behavior of R_1^H for CsSiH₃ strongly deviates from that predicted by the standard theory. First, the high-temperature slope of the ln R_1^H vs. T^{-1} peak appears to be much steeper than the low-temperature
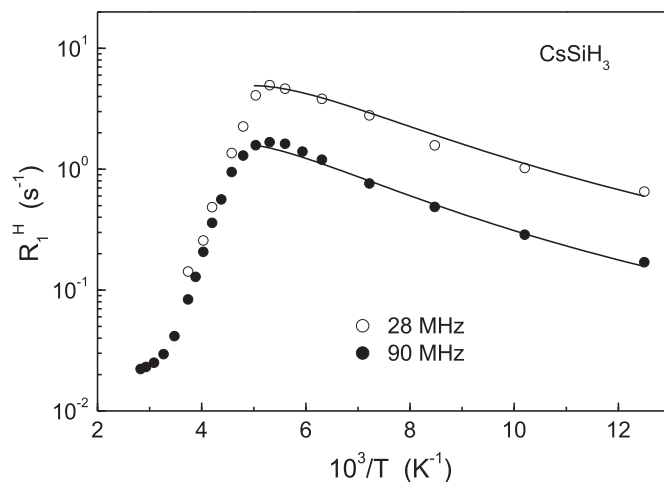
Fig. 4. Proton spin-lattice relaxation rates measured at 28 and 90 MHz for CsSiH₃ as functions of the inverse temperature. The solid lines show the simultaneous fit of the model with a Gaussian distribution of the activation energies to the data in the range 80–200 K.

one. Second, the observed frequency dependence of R_1^H at the low-temperature slope is considerably weaker than the predicted ω^{-2} dependence. Furthermore, there are certain deviations from the linear behavior of the $\ln R_1^H$ vs. T^{-1} plot both at high and low temperatures. The most evident reason for the unusual behavior of the proton spin-lattice relaxation rate in $CsSiH_3$ is the $\beta \rightarrow \alpha$ phase transition accompanied by the strong acceleration of the reorientational motion of SiH_3 groups. This phase transition in $CsSiH_3$ was studied both by neutron diffraction and quasielastic neutron scattering [16]. According to the QENS data [16], in the heating regime (corresponding to our present NMR measurements), the most pronounced changes in τ^{-1} occur between 200 K and 300 K. Because of this phase transition, the steep high-temperature slope of the $R_1^H(T)$ peak cannot be described in terms of regular thermally-activated changes in τ^{-1}; this slope should reflect rapid changes in the H jump rate due to the phase change. It is interesting to note that in some complex hydrides the order-disorder phase transitions lead to abrupt changes in R_1^H; for example, the order-disorder transition in sodium *closo*-hydroborate $Na_2B_{12}H_{12}$ near 520 K is accompanied by the two-orders-of-magnitude drop of R_1^H over the temperature interval of 5 K [13]. For $CsSiH_3$, the relaxation rate drop is not so sharp; this may be related to specific features of the $\beta - \alpha$ phase transitions in $MSiH_3$ occurring via intermediate phases [8,16]. The presence of disordered α-like nanodomains at temperatures much lower than the phase transition points was first reported for $KSiH_3$ and $RbSiH_3$ [8]. Because of their small size (2−4 nm [8]), these nanodomains may be invisible in diffraction experiments. The comprehensive QENS results for $CsSiH_3$ [16] are consistent with the presence of a nanostructured intermediate phase (*i*-phase) with the distinct reorientational dynamics being much faster than that for the β-phase, but slower than that for the α-phase. According to the QENS data [16], the α-, i-, and β-phases in $CsSiH_3$ can coexist over the temperature range of at least 170−250 K.

The complex behavior of $CsSiH_3$ related to the order-disorder phase transition prevents us from any attempts to parametrize the $R_1^H(T)$ data over the entire temperature range studied. Therefore, we have only tried to parametrize the $R_1^H(T)$ data at low temperatures ($T < 200$ K), where the β-phase is expected to be the dominant one. As noted above, the observed frequency dependence of the proton spin-lattice relaxation rate at the low-T slope of the $R_1^H(T)$ peak is considerably weaker than the ω^{-2} dependence. This feature is consistent with the presence of a certain distribution of H jump rates [29]. For parametrization of our low-temperature $R_1^H(T)$ data, we have used the simplest model based on a Gaussian distribution of the activation energies [29]; for this model, the observed relaxation rate is expressed as

$$R_1^H = \int R_1^H(E_a) G(E_a, \overline{E}_a, \Delta E_a) dE_a \tag{2}$$

Here $G(E_a, \overline{E}_a, \Delta E_a)$ is a Gaussian distribution function centered on $\overline{E}_a$ with the dispersion ΔE_a, and $R_1^H(E_a)$ is determined by combining the standard expression that relates the relaxation rate and τ,

$$R_1^H(E_a) = \frac{2\Delta M_{HH}\tau}{3}\left[\frac{1}{1+\omega^2\tau^2} + \frac{4}{1+4\omega^2\tau^2}\right], \tag{3}$$

and the Arrhenius law (Eq. (1)). It should be noted that all the known expressions for the proton relaxation rate due to the reorientational motion (including a number of exact solutions for some simple types of reorientations [26]) show the same functional form

of dependence on τ and ω, as Eq. (3). The parameters of the model are the average activation energy $\overline{E}_a$, the dispersion ΔE_a, the pre-exponential factor τ_0 and the amplitude factor ΔM_{HH} determined by the strength of the fluctuating part of dipole-dipole interaction between protons. The contribution of dipole-dipole $^1H-^{133}Cs$ interactions to the proton relaxation rate in $CsSiH_3$ can be neglected, since these interactions give only 2.6% of the total calculated 'rigid-lattice' second moment of the ^1H NMR line. The model parameters have been varied to find the best fit between the model $R_1^H(T)$ and the experimental data for $T < 200$ K at two resonance frequencies *simultaneously*. The results of such a simultaneous fit are shown by the solid curves in Fig. 4; the corresponding fit parameters: $\overline{E}_a = 226$ (8) meV, $\Delta E_a = 78$ (4) meV, $\tau_0 = 3.7(5) \times 10^{-15}$ s, and $\Delta M_{HH} = 3.4(1) \times 10^9$ s^{-2}. Note that the resulting fluctuating part of the second moment, ΔM_{HH}, corresponds to ~65% of the calculated 'rigid-lattice' second moment (see above); this is close to the expected 'intramolecular' value (75%) [14,28] for the case of uniaxial rotation of SiH_3 groups around the 3-fold symmetry axis.

The distribution width ΔE_a resulting from the fit appears to be rather large (about one-third of $\overline{E}_a$). This feature may indicate the presence of an additional jump process not resolved in the spin-lattice relaxation measurements. Indeed, if the difference between two frequency scales of H jump motion is relatively small (about one order of magnitude), an additional jump process may contribute only to the low-temperature slope of the single-peak $R_1^H(T)$ dependence that mimics the typical behavior for the model with a continuous jump rate distribution. Similar behavior of $R_1^H(T)$ was reported for a number of systems with two frequency scales of H jump motion, including some Laves-phase hydrides [30] and the ordered *closo*-hydroborate salt $Rb_2B_{10}H_{10}$ [31]. The presence of an additional jump process in the temperature range, where the β-phase is expected to be the dominant one, is also consistent with recent QENS results for $CsSiH_3$ [16]. These results indicate that the description of the elastic incoherent structure factor measured on the backscattering neutron spectrometer at 200 K in terms of the model of 3-fold SiH_3 reorientations (the only physically reasonable model for the ordered β-phase) requires an extra contribution (43%) to the elastic peak intensity. Such a large extra contribution to the elastic peak intensity is consistent [16] with the presence of H atoms moving much faster than those in the β-phase. However, we have not tried to use a two-peak distribution of the activation energies for parametrization of our low-T relaxation rate data, since this would require an introduction of a number of additional fit parameters.

The observed change in the high-temperature slope of the $\ln R_1^H$ vs. T^{-1} plot near 300 K (see Fig. 4) can be attributed to the upper boundary of the phase transition region. This interpretation implies the existence of a single α-phase of $CsSiH_3$ above 300 K, so that the behavior of R_1^H at $T > 300$ K should be governed by the regular Arrhenius temperature dependence of τ. The activation energy for H jump motion in this temperature range can be directly estimated from the proton spin-lattice relaxation data, since in the limit of fast motion (see above) R_1^H is proportional to τ. The estimate based on an Arrhenius approximation of our $R_1^H(T)$ data in the range 324−354 K gives the activation energy of 41(4) meV. This value is close to the activation energy for α-phase of $CsSiH_3$ (48(2) meV) found from QENS experiments [16].

3.2. ^{133}Cs NMR spectra and spin-lattice relaxation rates

The evolution of the ^{133}Cs NMR spectra for $CsSiH_3$ with temperature is shown in Fig. 5. As in the case of the proton NMR spectra, with increasing temperature we observe a considerable
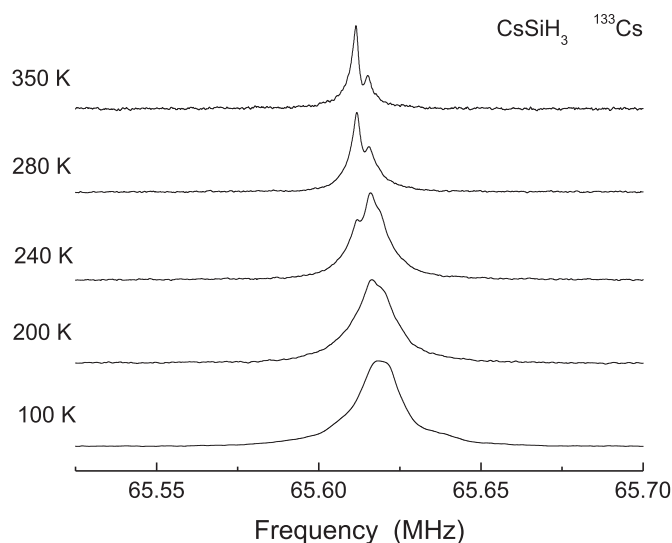
Fig. 5. Evolution of the ^{133}Cs NMR spectrum for CsSiH$_3$ with temperature.

narrowing of the ^{133}Cs spectra accompanied by changes in their shape. The temperature dependence of the ^{133}Cs NMR line width Δ_{Cs} (full width at half-maximum) is shown in Fig. 6. Note that the onset of the order-disorder phase transition (in the temperature range 200−260 K) only slightly affects the value of Δ_{Cs}; this is consistent with the localized nature of H motion. In the studied temperature range of 100−350 K, the most pronounced drop of Δ_{Cs} is observed between 260 K and 300 K, and at $T > 300$ K, the line width reaches a plateau. Such a behavior is typical of the case of diffusing cations in ionic conductors (see, for example, the "steps" in ^{7}Li NMR line widths in Refs. [32−34]). It should be noted, however, that the presence of a certain structure of the ^{133}Cs NMR spectrum for CsSiH$_3$ at 350 K suggests that the ^{133}Cs electric quadrupole interaction is not fully averaged out at this temperature. It is extremely difficult to simulate NMR line shapes in situations when a quadrupole interaction is partially averaged by atomic motion. Furthermore, we cannot exclude a possibility of multiple Cs sites characterized by different shifts. Similar results were reported for ^{23}Na NMR spectra in Na$_2$(BH$_4$) (NH$_2$) showing fast Na$^+$ diffusion [35]. For CsSiH$_3$, we have to distinguish between

the effects due to the reorientational H motion and the diffusive motion of Cs$^+$ cations. For this purpose, we can use the results of the ^{133}Cs spin-lattice relaxation rate measurements shown in Fig. 7.

Comparison of Figs. 7 and 4 indicates that below 300 K, the behavior of the ^{133}Cs spin-lattice relaxation rate R_1^{Cs} resembles that of R_1^H. In particular, the $R_1^{Cs}(T)$ peak is observed at nearly the same temperature as the $R_1^H(T)$ peak. Furthermore, the low-temperature slope of the $R_1^{Cs}(T)$ peak is close to that of the $R_1^H(T)$ peak. Thus, the observed ^{133}Cs relaxation rate peak can be attributed to the reorientational motion of SiH$_3$ groups that modulates the relatively weak ^{133}Cs − ^{1}H dipole-dipole interaction. This is supported by the small amplitude of the $R_1^{Cs}(T)$ peak (0.36 s^{-1}) which is two orders of magnitude lower than the amplitude of the $R_1^H(T)$ peak. Such a difference in the maximum values of the spin-lattice relaxation rates is in general agreement with the estimated contributions of ^{133}Cs − ^{1}H and ^{1}H − ^{1}H dipole-dipole interactions to the corresponding second moments. It should be noted that reorientational jumps of SiH$_3$ groups are not expected to add any electric quadrupole contribution to the ^{133}Cs relaxation rate, since each reorientational jump does not change the charge configuration around Cs sites. In contrast to the case of the electric quadrupole interaction, the dipole-dipole interaction is *pairwise*, i.e., any changes in the radius vector connecting a pair of interacting nuclear spins should contribute to the nuclear spin relaxation. It can be concluded that the behavior of the ^{133}Cs spin-lattice relaxation rate below 300 K is governed by the reorientational motion of SiH$_3$ groups via ^{133}Cs − ^{1}H dipole-dipole interactions.

Above 300 K, the ^{133}Cs relaxation rate starts to increase with increasing temperature (Fig. 7). This behavior of R_1^{Cs} differs qualitatively from that of R_1^H in the same temperature range (Fig. 4); it is consistent with the onset of an additional low-frequency jump process, such as diffusive jumps of Cs$^+$ ions. It should be noted that R_1^{Cs} starts to increase at temperatures just above the characteristic "step" in the line width Δ_{Cs} (Fig. 6). This feature is typical of the onset of cation diffusive motion on the NMR frequency scale [32−34]; it corresponds to the case when the cation jump rate is higher than ~10^4 s^{-1} (sufficient to cause the NMR line narrowing), but is still considerably lower than ~10^8 s^{-1} (not reaching a new relaxation rate maximum).

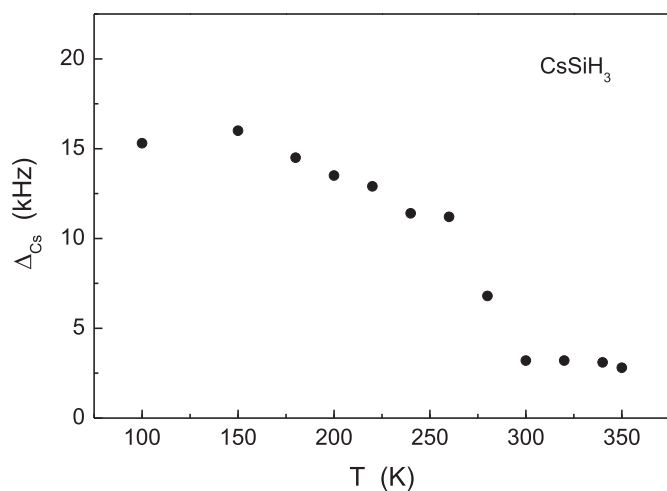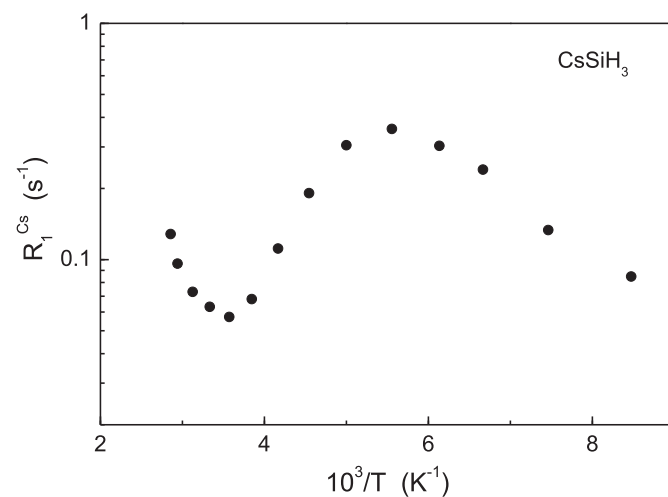**Fig. 6.** Temperature dependence of the width (full width at half-maximum) of the ^{133}Cs NMR spectrum measured for CsSiH$_3$ at 65.62 MHz.

Fig. 7. ^{133}Cs spin-lattice relaxation rate measured at 65.62 MHz for CsSiH$_3$ as a function of the inverse temperature.

4. Conclusions

The results of our proton NMR measurements indicate that $[SiH_3]^-$ groups in $CsSiH_3$ retain unusually high reorientational mobility down to low temperatures. According to the ^{1}H NMR line width measurements, even at $T = 14$ K the jump rate of SiH_3 reorientations in $CsSiH_3$ is about 10^5 s^{-1}. In agreement with recent QENS results for $CsSiH_3$ [16], our proton spin-lattice relaxation data are consistent with a coexistence of at least two reorientational jump processes below 200 K. The order-disorder ($\beta \rightarrow \alpha$) phase transition accompanied by the strong acceleration of SiH_3 reorientations and by the change in the reorientational mechanism leads to the considerable drop of the measured ^{1}H spin-lattice relaxation rate R_1^H; however, this drop is not as abrupt as in the case of the order-disorder transitions in borohydrides [36] and *closo*-hydroborates [13]. The smearing of the R_1^H "step" in the phase transition region for $CsSiH_3$ suggests that the order-disorder transition in this compound occurs via the formation of an intermediate phase [16]. For the high-temperature disordered α-phase of $CsSiH_3$, the activation energy for SiH_3 reorientations estimated from our $R_1^H(T)$ data is 41(4) meV. The [133]Cs NMR results are consistent with the onset of diffusive motion of Cs^+ ions at the frequency scale of $\sim 10^4$ s^{-1} above 300 K.

Acknowledgements

References

[1] J.-N. Chotard, W.S. Tang, P. Raybaud, R. Janot, Chem. Eur J. 17 (2011) 12302–12309.
[2] W.S. Tang, J.-N. Chotard, P. Raybaud, R. Janot, Phys. Chem. Chem. Phys. 14 (2012) 13319–13324.
[3] W.S. Tang, J.-N. Chotard, P. Raybaud, R. Janot, J. Phys. Chem. C 118 (2014) 3409–3419.
[4] A. Jain, T. Ichikawa, S. Yamaguchi, H. Miyaoka, Y. Kojima, Phys. Chem. Chem. Phys. 16 (2014) 26163–26167.
[5] R. Janot, W.S. Tang, D. Clémençon, J.-N. Chotard, J. Mater. Chem. A 4 (2016) 19045–19052.
[6] O. Mundt, G. Becker, H.-M. Hartmann, W. Schwarz, Z. Anorg. Allg. Chem. 572 (1989) 75–88.
[7] W.S. Tang, M. Dimitrievska, J.-N. Chotard, W. Zhou, R. Janot, A.V. Skripov, T.J. Udovic, J. Phys. Chem. C 120 (2016) 21218–21227.
[8] R. Nedumkandathil, A. Jaworski, A. Fischer, C. Österberg, Y.-C. Lin, M. Karlsson, J. Grins, A.J. Pell, M. Edén, U. Häussermann, J. Phys. Chem. C 121 (2017) 5241–5252.
[9] A.V. Skripov, A.V. Soloninin, O.A. Babanova, R.V. Skoryunov, J. Alloys Compd. 645 (2015) S428–S433.
[10] E.G. Sorte, S.B. Emery, E.H. Majzoub, T. Ellis-Caleo, Z.L. Ma, B.A. Hamman, S.E. Hayes, R.C. Bowman, M.S. Conradi, J. Phys. Chem. C 118 (2014) 5725–5732.
[11] M. Müller, B. Asmussen, W. Press, J. Senker, H. Jacobs, H. Büttner, H. Schober, J. Chem. Phys. 109 (1998) 3559–3567.
[12] A. Gradišek, L.H. Jepsen, T.R. Jensen, M.S. Conradi, J. Phys. Chem. C 120 (2016) 24646–24654.
[13] A.V. Skripov, O.A. Babanova, A.V. Soloninin, V. Stavila, N. Verdal, T.J. Udovic, J.J. Rush, J. Phys. Chem. C 117 (2013) 25961–25968.
[14] E. Weiss, G. Hencken, H. Kühr, Chem. Ber. 103 (1970) 2868–2872.
[15] C. Österberg, H. Fahlquist, U. Häussermann, C.M. Brown, T.J. Udovic, M. Karlsson, J. Phys. Chem. C 120 (2016) 6369–6376.
[16] M. Dimitrievska, J.-N. Chotard, R. Janot, A. Faraone, W.S. Tang, A.V. Skripov, T.J. Udovic, J. Phys. Chem. C 122 (2018) 23985–23997.
[17] B. Bonnetot, H. Mongeot, A. Aboukhassib, F. Lefebvre, Inorg. Chim. Acta. 193 (1992) 21–26.
[18] N. Verdal, J.-H. Her, V. Stavila, A.V. Soloninin, O.A. Babanova, A.V. Skripov, T.J. Udovic, J.J. Rush, J. Solid State Chem. 212 (2014) 81–91.
[19] T.J. Udovic, M. Matsuo, W.S. Tang, H. Wu, V. Stavila, A.V. Soloninin, R.V. Skoryunov, O.A. Babanova, A.V. Skripov, J.J. Rush, A. Unemoto, H. Takamura, S. Orimo, Adv. Mater. 26 (2014) 7622–7626.
[20] T.J. Udovic, M. Matsuo, A. Unemoto, N. Verdal, V. Stavila, A.V. Skripov, J.J. Rush, H. Takamura, S. Orimo, Chem. Commun. 50 (2014) 3750–3752.
[21] W.S. Tang, M. Matsuo, H. Wu, V. Stavila, W. Zhou, A.A. Talin, A.V. Solininin, R.V. Skoryunov, O.A. Babanova, A.V. Skripov, A. Unemoto, S. Orimo, T.J. Udovic, Adv. Energy Mater. 6 (2016), 1502237.
[22] Z. Lu, F. Giucci, J. Mater. Chem. A 4 (2016) 17740–17748.
[23] J.B. Varley, K. Kweon, P. Mehta, P. Shea, T.W. Heo, T.J. Udovic, V. Stavila, B.C. Wood, ACS Energy Lett. 2 (2017) 250–255.
[24] M. Dimitrievska, P. Shea, K. Kweon, M. Bercx, J.B. Varley, W.S. Tang, A.V. Skripov, V. Stavila, T.J. Udovic, B.C. Wood, Adv. Energy Mater. 8 (2018) 1703422.
[25] The mention of all commercial suppliers in this paper is for clarity and does not imply the recommendation or endorsement of these suppliers by NIST.
[26] A. Abragam, The Principles of Nuclear Magnetism, Clarendon Press, Oxford, 1961.
[27] A.J. Horsewill, Prog. Nucl. Magn. Reson. Spectrosc. 35 (1999) 359–389.
[28] J.M. Dereppe, J. Chem. Phys. 58 (1973) 1254–1255.
[29] J.T. Markert, E.J. Cotts, R.M. Cotts, Phys. Rev. B 37 (1988) 6446–6452.
[30] A.V. Skripov, Defect Diffusion Forum 224–225 (2003) 75–92.
[31] M. Dimitrievska, V. Stavila, A.V. Soloninin, R.V. Skoryunov, O.A. Babanova, H. Wu, W. Zhou, W.S. Tang, A. Faraone, J.D. Tarver, B.A. Trump, A.V. Skripov, T.J. Udovic, J. Phys. Chem. C 122 (2018) 15198–15207.
[32] V. Epp, Ö. Gün, H.-J. Deiseroth, M. Wilkening, J. Phys. Chem. Lett. 4 (2013) 2118–2123.
[33] A.V. Skripov, A.V. Soloninin, M.B. Ley, T.R. Jensen, Y. Filinchuk, J. Phys. Chem. C 117 (2013) 14965–14972.
[34] A.V. Skripov, R.V. Skoryunov, A.V. Soloninin, O.A. Babanova, M. Matsuo, S. Orimo, J. Phys. Chem. C 119 (2015) 13459–13464.
[35] A.V. Soloninin, O.A. Babanova, E.Y. Medvedev, A.V. Skripov, M. Matsuo, S. Orimo, J. Phys. Chem. C 118 (2014) 14805–14812.
[36] O.A. Babanova, A.V. Soloninin, A.P. Stepanov, A.V. Skripov, Y. Filinchuk, J. Phys. Chem. C 114 (2010) 3712–3718.